

See discussions, stats, and author profiles for this publication at: <https://www.researchgate.net/publication/259718511>

# Rapid Identification of Keap1–Nrf2 Small-Molecule Inhibitors through Structure-Based Virtual Screening and Hit-Based Substructure Search

ARTICLE in JOURNAL OF MEDICINAL CHEMISTRY · JANUARY 2014

Impact Factor: 5.45 · DOI: 10.1021/jm4017174 · Source: PubMed

CITATIONS

20

READS

104

## 5 AUTHORS, INCLUDING:



**Chunlin Zhuang**

Second Military Medical University, Shanghai

24 PUBLICATIONS 158 CITATIONS

SEE PROFILE



**Wannian Zhang**

Second Military Medical University, Shanghai

83 PUBLICATIONS 1,199 CITATIONS

SEE PROFILE



**Yuk Y Sham**

University of Minnesota Twin Cities

60 PUBLICATIONS 2,186 CITATIONS

SEE PROFILE



**Chengguo Xing**

University of Minnesota Twin Cities

63 PUBLICATIONS 725 CITATIONS

SEE PROFILE

# Rapid Identification of Keap1–Nrf2 Small-Molecule Inhibitors through Structure-Based Virtual Screening and Hit-Based Substructure Search

Chunlin Zhuang,<sup>†,‡</sup> Sreekanth Narayanapillai,<sup>†</sup> Wannian Zhang,<sup>‡</sup> Yuk Yin Sham,<sup>\*,§</sup> and Chengguo Xing<sup>\*,†</sup>

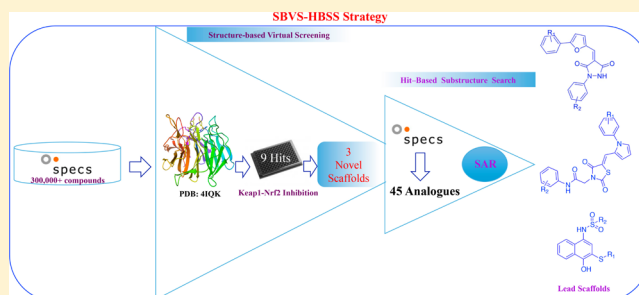
<sup>†</sup>Department of Medicinal Chemistry, University of Minnesota, 2231 Sixth Street SE, Minneapolis, Minnesota 55455, United States

<sup>‡</sup>Department of Medicinal Chemistry, Second Military Medical University, 325 Guohe Road, Shanghai 200433, People's Republic of China

<sup>§</sup>Center for Drug Design, University of Minnesota, 516 Delaware Street SE, Minneapolis, Minnesota 55455, United States

## **S** Supporting Information

**ABSTRACT:** In this study, rapid structure-based virtual screening and hit-based substructure search were utilized to identify small molecules that disrupt the interaction of Keap1–Nrf2. Special emphasis was placed toward maximizing the exploration of chemical diversity of the initial hits while economically establishing informative structure–activity relationship (SAR) of novel scaffolds. Our most potent non-covalent inhibitor exhibits three times improved cellular activation in Nrf2 activation than the most active noncovalent Keap1 inhibitor known to date.



## ■ INTRODUCTION

Oxidative stress can lead to chronic inflammation, which is crucial to the development of many diseases, including cancer, cardiovascular, and neurodegenerative diseases.<sup>1</sup> Antioxidant defense system is one of the major mechanisms to protect cells from such stress. A number of enzymes, such as NADPH:quinone oxidoreductase 1 (NQO-1), heme oxygenase-1 (HO-1), superoxide dismutase (SOD), and glutathione S-transferase (GST),<sup>2</sup> are the key components of this system. They are mainly regulated by three cellular components: Kelch-like ECH-associated protein 1 (Keap1), nuclear factor erythroid 2-related factor 2 (Nrf2) and antioxidant response elements (ARE).<sup>3</sup> Under unstressed conditions, Nrf2 remains at low cellular concentration and is negatively regulated by Keap1 mediated proteasomal degradation.<sup>3</sup> Upon exposure to oxidative stress, Keap1 is deactivated. Nrf2 escapes Keap1-mediated degradation, resulting in its nuclear translocation and transcriptional activation of the ARE dependent genes, including the above-mentioned entities. Thus, targeting the Keap1–Nrf2–ARE signaling pathway is one logical strategy to discover therapeutic agents for diseases and conditions involving oxidative stress.<sup>4</sup> To date, most Nrf2 activators, including natural products (e.g., sulforaphane and curcumin) and synthetic compounds (e.g., oltipraz and bardoxolone methyl), target this pathway through covalent modification and deactivation of Keap1 protein via its reactive cysteine residues.<sup>4,5</sup> Direct inhibition of the Keap1–Nrf2 protein–protein interactions via a non-covalent mechanism is an alternative for the discovery of small-molecule Nrf2 activators with potential advantages such as lower toxicity.<sup>4</sup>

Human Keap1 is a 70 kDa protein<sup>6</sup> containing five domains: (a) N-terminal region (NTR), (b) BTB (broad complex, tramtrack, and Bric a brac), an evolutionarily conserved protein–protein interaction motif that dimerizes with Cullin 3 (Cul3)-based ubiquitin E3 ligase complex for Nrf2 ubiquitination; (c) intervening region (IVR), a cysteine-rich region; (d) double glycine region (DGR), a domain that comprises six-bladed Kelch motifs and binds to the Neh2 domain of Nrf2;<sup>7,8</sup> and (e) C-terminal region (CTR). Human Nrf2 has 605 amino acid residues that form six conserved domains: Neh1–Neh6. Each domain has its own biological function, particularly the N-terminus Neh2 domain, which contains two regions that bind to Keap1 Kelch domain.<sup>8</sup> One region (amino acids 17–32) contains a DLG motif with a low binding affinity ( $K_D \approx 1000$  nM).<sup>7</sup> Another region (amino acids 77–82) contains an ETGE motif with a high binding affinity ( $K_D \approx 5.3$  nM).<sup>9</sup> On the basis of these two motifs, several peptides disrupting the Keap1–Nrf2 interaction have been developed. Unfortunately, their efficacy has not been proven at the cellular level, probably due to poor cell penetration.<sup>10</sup>

Subsequently, the discovery of non-peptide Keap1–Nrf2 inhibitors has emerged. One recent study<sup>11</sup> reported the discovery of a potent small-molecule inhibitor **1** ( $K_i = 1.0$   $\mu$ M, Figure 1) via a high throughput screening of NIH MLPCN library of 337116 compounds (PubChem BioAssay ID: 504523, 504540) and hit optimization. This compound showed decent

**Received:** November 7, 2013

**Published:** January 13, 2014

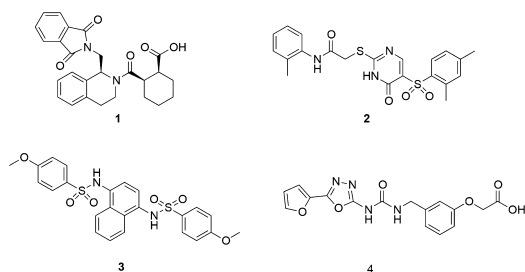


**Figure 1.** Recently published small molecule inhibitors of Keap1–Nrf2 interaction.

ARE-inducing activity with an  $EC_{50}$  of  $18\ \mu\text{M}$  in a cell-based functional assay. Another high throughput screening study<sup>12</sup> reported two novel scaffolds (2 and 3). Compound 3 (PDB entry: 4IQK) showed a good binding inhibition ( $IC_{50} = 2.7\ \mu\text{M}$ ), while compound 2 (PDB entry: 4IN4) was rather weak ( $IC_{50} = 118\ \mu\text{M}$ ). Compound 3 was demonstrated to up-regulate Nrf2 target gene NQO1 and stabilize Nrf2 protein using an ARE-driven luciferase reporter system in DLD1 cells. A small molecule 4 has been recently released in PDB bank (PDB entry: 3VNG, 3VNH). Comparison of these four crystal structures showed that all ligands bind to the same protein–protein interfacial pocket with minimal allosteric distortion of the local side chains (Supporting Information Figure S3). This provides a strong structural basis for in silico screening studies by using a single X-ray crystallographic structure as a starting point. Inhibitors with novel scaffolds are expected to complement current leads for future translational development.

Structure-based virtual screening (SBVS) and hit-based substructure search (HBSS) are powerful tools for drug discovery.<sup>13–15</sup> In this study, we successfully identified novel Keap1–Nrf2 inhibitors with informative SARs by employing an integrated SBVS and HBSS approach.

## RESULTS AND DISCUSSION

**Design Rationale.** In this study, in-house synthesis was replaced by taking the advantage that compounds in many commercial chemical databases are inherently enriched with analogues defined by the nature of their synthetic routes. Thus, an SAR of the hits identified through SBVS can easily be established through subsequent extraction of analogues of the same chemotype within the same database. This approach is economical and highly efficient to achieve a preliminary SAR for large numbers of chemically diverse hits prior to focused medicinal chemistry exploration. It is a standard best practice for efficiently exploring commercial compound databases.

**Structure-Based Virtual Screening.** A schematic of the overall virtual screening procedure in this study is presented in Supporting Information Figure S1. Specs database (>300000 compounds) was processed, resulting in a screening library of 153611 compounds with  $>10^6$  conformations. Virtual screening was carried out using Schrodinger's Glide in three steps, each with increasing level of computational sampling and precision, resulting in 90 compounds with Glidescore less than that of compound 3. While Glidescore performs poorly in the estimation of binding affinity,<sup>16</sup> it is commonly used as one of the matrices for selecting poses in SBVS. To ensure maximum chemical diversity and to limit redundancy in our initial testing, these compounds were subjected to structure similarity comparison and clustering based on their calculated Tanimoto coefficient using the 2D fingerprint.<sup>17</sup> The selected

65 compounds, representing 61 novel structural clusters with Tanimoto coefficient  $<0.8$ , were purchased from the commercial source (details in Supporting Information) for biological evaluation.

**Disrupting the Binding of Keap1–Nrf2.** The inhibitory activity ( $K_{D2}$ ) of the 65 selected compounds from SBVS were measured by an established fluorescence anisotropy assay.<sup>18</sup> On the basis of its low micromolar inhibition activity, availability of X-ray cocrystallographic structure, and ease of synthesis, compound 3 was chosen as our reference compound. All compounds were first evaluated at  $100\ \mu\text{M}$ , and 24 showed detectable or decent Keap1–Nrf2 inhibition (Supporting Information Table S1). These compounds were then evaluated to determine the  $K_{D2}$ . Nine possessed good inhibitory activity, with  $K_{D2}$  ranging from  $2.9$  to  $75.48\ \mu\text{M}$  (Figure 2).

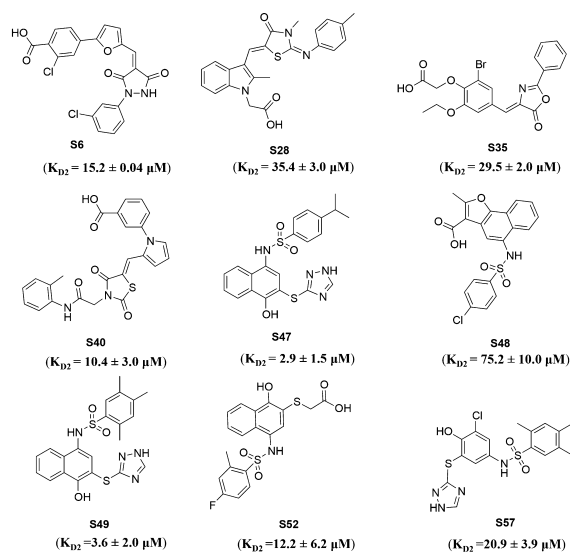


**Figure 2.** Chemical structures and Keap1–Nrf2 inhibitory activities of the hits from structure-based virtual screening.

Interestingly, the phenylsulfonic amide turned out to be a common scaffold (S47, S48, S49, S52, and S57), which was different from the earlier reported inhibitors. Among the identified hits, compounds S47 and S49 displayed excellent Keap1–Nrf2 inhibitory activity, with  $K_{D2}$  values of  $2.9$  and  $3.6\ \mu\text{M}$  respectively, comparable to that of the reference compound 3 ( $K_{D2} = 3.3 \pm 0.5\ \mu\text{M}$ , Supporting Information Figure S12) in our assay. Compound S6 and S40 showed moderate inhibitory activity, with  $K_{D2}$  values of  $15.2$  and  $10.4\ \mu\text{M}$ . To obtain further insight that would guide the hit-based substructure search, the docking modes of these compounds with the Keap1 Kelch domain were re-examined.

From the observed binding poses of our docking studies (Figure 3 and Supporting Information S6), three recurring features were observed that may play an important role in selective binding of noncovalent Keap1 inhibitors, namely (a)  $\pi$ –cation interaction of its aromatic scaffold with Arg415, (b) hydrogen bonds with Ser363, Ser508, or Ser555, and (c) salt bridge interaction between our negatively charged triazole or acetate groups with surface Arg380, Arg415, or Arg483. Interestingly, the most active and structurally similar compounds, S47 and 3, involved a very different mode of binding with deep insertion of their aromatic scaffold (cumenyl of S47 and naphthyl of compound 3) into the cationic Arg415 pocket.

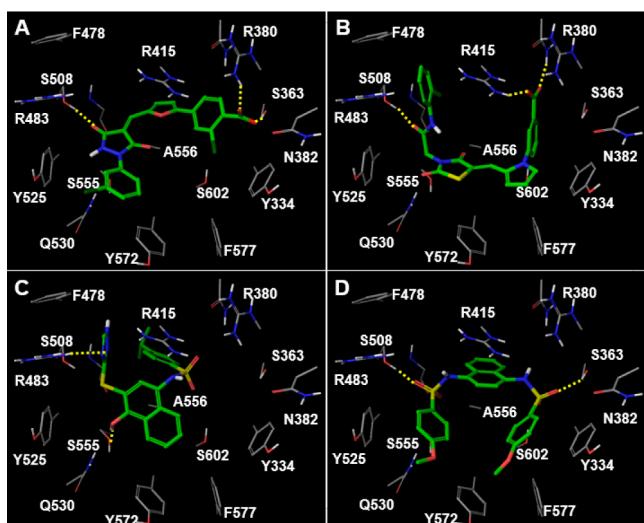


**Figure 3.** Potential binding modes of the lead compounds (A) S6, (B) S40, (C) S47, and (D) 3 with the Keap1 Kelch domain.

The differences are likely due to the fact that compound 3 is structurally symmetric and electroneutral while S47 is not. The strong salt bridge interaction of S47 is also accompanied by compensated replacement of the naphthyl group by the cumenyl group inside Arg415 pocket (Figure 3C). The structurally symmetric compound 3, on the other hand, binds in a more symmetric way in relation to the 6-bladed fold symmetry of the protein, involving two sulfonamide groups and a 4-methoxyphenyl group, which formed additional hydrogen bonds with Ser363 and Ser508 and  $\pi$ - $\pi$  interactions with Tyr334 to compensate for its potency (Figure 3D).

#### Hit-Based Substructure Search and Preliminary SARs.

Three scaffolds (S6, S40, and S47) representing novel chemotypes for Keap1–Nrf2 inhibitors were selected for hit-based substructure search in Specs database. Nine analogues of S6, 13 analogues of S40, and 23 analogues of S47 were selected and purchased for biological evaluation (25 of them have been confirmed in-house for their identity and purity by NMR, MS, and HPLC with details in Supporting Information).

The fluorescence anisotropy assay revealed that four compounds (HS1, HS5, HS8, and HS9) within S6 series (Table 1) possessed moderate potency. SAR analysis revealed that decreased inhibitory activity was observed for non-halogen substituted derivative HS1 ( $K_{D2} = 42.9 \pm 2.6 \mu\text{M}$ ) compared to the halogen-substituted one, S6 ( $K_{D2} = 15.2 \pm 0.04 \mu\text{M}$ ), highlighting the importance of substitutions on R<sub>2</sub> group. No substitution on R<sub>1</sub> (HS3) was totally inactive. Introducing amide (HS7) or sulphonamide (HS2, HS4, and HS6) reduced the inhibitory activity. Disubstitution on the same benzene ring (S6) exhibited higher inhibition than the mono ones (HS8).

For the S40 series (Table 2), the carboxyl group on R<sub>1</sub> was critical for the inhibitory activity, likely because it may form hydrogen bonds with Arg380 and Arg415. The corresponding hydroxyl (HS18) or methoxy groups (HS12 and HS19) were completely inactive. Compounds with various substitutions on R<sub>2</sub> position also showed quite different inhibitory activity. The methyl derivatives (S40, HS10, HS11, and HS13) were better than the halogen derivatives (HS15 and HS16). When the methyl group on position 2 (S40) was moved to position 3 (HS10), decreased activity was observed. Similarly, disubstitution on the same benzene ring (HS11, HS13, and HS14) led to

**Table 1.** Inhibitory Activity of Compounds HS1–HS9 for Keap1–Nrf2 Binding

Compounds	R <sub>1</sub>	R <sub>2</sub>	K <sub>D2</sub> ( $\mu\text{M}$ )
S6	3-Cl-4-COOH	3-Cl	15.2 $\pm$ 0.04
HS1	3-Cl-4-COOH	H	42.9 $\pm$ 2.6
HS2	4-SO <sub>2</sub> NH <sub>2</sub>	4-COOCH <sub>3</sub>	>100
HS3	H	4-Br	>100
HS4	4-SO <sub>2</sub> NH <sub>2</sub>	3-CH <sub>3</sub>	>100
HS5	4-COOH	3-F	77.8 $\pm$ 5.1
HS6	4-SO <sub>2</sub> NH <sub>2</sub>	4-CH <sub>3</sub>	>100
HS7	4-CONH <sub>2</sub>	4-F	>100
HS8	3-COOH	3-Cl	49.2 $\pm$ 6.9
HS9	2-COOH-4-Br	3-Cl	39.54 $\pm$ 7.6

**Table 2.** Inhibitory Activity of Compounds HS10–HS21 for Keap1–Nrf2 Binding

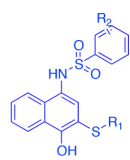
Compounds	R <sub>1</sub>	R <sub>2</sub>	K <sub>D2</sub> ( $\mu\text{M}$ )
S40	3-COOH	2-CH <sub>3</sub>	10.4 $\pm$ 3.0
HS10	3-COOH	3-CH <sub>3</sub>	68.2 $\pm$ 6.8
HS11	3-COOH	2,4-2CH <sub>3</sub>	47.6 $\pm$ 8.9
HS12	4-OCH <sub>3</sub>	4-CH <sub>3</sub>	>100
HS13	3-COOH	3,4-2CH <sub>3</sub>	28.9 $\pm$ 1.6
HS14	3-COOH	2,6-2CH <sub>3</sub>	>100
HS15	3-COOH	4-Cl	>100
HS16	3-COOH	4-F	>100
HS17	4-COOH	4-OCH <sub>3</sub>	23.8 $\pm$ 2.5
HS18	4-OH	2-F	>100
HS19	4-OCH <sub>3</sub>	3-CH <sub>3</sub>	>100
HS20			>100
HS21			>100

decreased activity compared to the monosubstituted derivative S40. Removing either of the two benzene rings (HS20 and HS21) showed decreased activity.

The inhibitory activity of S47 analogues is summarized in Tables 3 and 4. Compounds S47, S49, HS26, HS27, HS28, HS31, HS39, and HS41 showed activity lower than 10  $\mu\text{M}$ . Notably, compounds S47, S49, HS26, HS31, and HS39 had  $K_{D2}$  values around 3  $\mu\text{M}$ , comparable to that of the reference compound 3 ( $K_{D2} = 3.3 \pm 0.5 \mu\text{M}$ ). The key observations of the SARs from these analogues have been summarized as follows: generally, the triazole derivatives were more potent than the carboxylates (Table 3). Introducing substituents on the NH group of triazole (HS33) or replacing the whole triazole by benzene rings (HS34–HS35) or other aromatic



Table 3. Inhibitory Activity of Compounds HS22–HS38 for Keap1–Nrf2 Binding

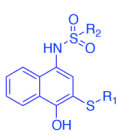


Compounds	R <sub>1</sub>	R <sub>2</sub>	K <sub>D2</sub> (μM)
S47		4-CH(CH <sub>3</sub> ) <sub>2</sub>	2.9 ± 1.5
S49		2,4,5-3CH <sub>3</sub>	3.6 ± 2.0
S52	-CH <sub>2</sub> COOH	2-CH <sub>3</sub> -4-F	12.2 ± 6.2
HS22	-CH <sub>2</sub> COOH	4-Br	14.7 ± 1.6
HS23	-CH <sub>2</sub> COOH	4-F	30.2 ± 2.6
HS24	-CH <sub>2</sub> COOH	4-Cl	15.3 ± 3.8
HS25	-CH <sub>2</sub> COOH	4-CH <sub>3</sub>	15.4 ± 0.9
HS26	-CH <sub>2</sub> COOH	2,4,6-3CH <sub>3</sub>	4.2 ± 0.4
HS27	-CH <sub>2</sub> COOH	4-CH(CH <sub>3</sub> ) <sub>2</sub>	6.4 ± 1.4
HS28		4-OCH <sub>3</sub>	6.8 ± 2.6
HS29		4-Br	13.1 ± 2.9
HS30		H	61.2 ± 5.4
HS31		4-OCH <sub>2</sub> CH <sub>3</sub>	3.1 ± 0.3
HS32		4-CH <sub>3</sub>	>100
HS33		H	55.5 ± 15.8
HS34		4-OCH <sub>3</sub>	>100
HS35		4-CH <sub>3</sub>	>100
HS36		4-CH <sub>3</sub>	>100
HS37		4-C(CH <sub>3</sub> ) <sub>3</sub>	>100
HS38		4-CH <sub>3</sub>	>100

rings (HS32 and HS36–HS38) dramatically reduced the inhibitory activity, presumably due to the loss of the salt bridge interaction with Arg483. A hydroxyl group was critical for the inhibitory activity because of the hydrogen bond interaction with the backbone of Ser555. Thus, acetylation of the hydroxyl group (HS43) or cyclization with sulfur (HS44) rendered the compounds completely inactive. As the compound with isopropylphenyl group (S47) could be inserted deeply into the central cavity of Keap1 protein, the derivative with no substitution on the benzene ring (HS30) had a poor inhibition ( $K_{D2} = 61.2 \pm 5.4 \mu\text{M}$ ). Introducing a methoxy group on position 4 (HS28) led to a more than 10-fold increase in activity. Ethoxyl derivative (HS31) also enhanced the activity with a  $K_{D2}$  value of  $3.1 \pm 0.3 \mu\text{M}$ .

The compounds with aliphatic groups (S47, S49, S52, HS25, HS27–HS28, and 31) on the benzene ring were more potent than the halogen substituted ones (HS22–HS24, HS29). Tri- or disubstituted analogues were more potent than the monosubstituted ones, such as HS26 (2,4,6-trimethyl,  $K_{D2} = 4.2 \pm 0.4 \mu\text{M}$ ), HS25 (4-methyl,  $K_{D2} = 15.4 \pm 0.9 \mu\text{M}$ ), and HS27 (4-isopropyl,  $K_{D2} = 6.4 \pm 1.4 \mu\text{M}$ ). Naphthyl (HS39) and quinolyl (HS40) were tolerated with similar activity compared with the phenyl ones (Table 4). The thienyl compound (HS42) was 10-fold less potent, probably

Table 4. Inhibitory Activity of Compounds HS39–HS45 for Keap1–Nrf2 Binding



Compounds	R <sub>1</sub>	R <sub>2</sub>	K <sub>D2</sub> (μM)
HS39			3.6 ± 0.5
HS40	-CH <sub>2</sub> COOH		18.9 ± 1.9
HS41	-CH <sub>2</sub> COOH		7.8 ± 1.7
HS42	-CH <sub>2</sub> COOH		36.6 ± 9.7
HS43			>100
HS44			>100
HS45			>100

potentially due to its insufficient occupation of the binding site. Removing one aromatic ring of the naphthyl (S57 and HS45) was unfavorable.

The most potent compounds (S6, S40, S47, and HS26) of each class were then confirmed to bind with Keap1 protein non-covalently in a reversible binding assay by reproducing similar binding affinities of dialyzed Keap1 to its fluorescence probe (Supporting Information Figure S13).

**Differential Scanning Fluorimetry (DSF) Assay.** The affinity of selected compounds to Keap1 protein was then confirmed by a qualitative orthogonal DSF assay at a single concentration used in previous validation studies for Keap1–Nrf2 inhibition.<sup>19,20</sup> One advantage of DSF is that it can be done with higher throughput without requiring large amounts of protein. As expected, compounds S47 and HS31 showed significant decrease ( $\Delta T_m = 5$  and  $4^\circ\text{C}$  respectively) in melting temperatures of Keap1 protein, while the reference compound 3 was not very sensitive in this assay (Figure 4 and Supporting Information Figure S14). The data also showed S6 and S40 with moderate potency only had 1 or  $2^\circ\text{C}$  difference compared to DMSO control, while the negative control compounds HS32 and HS44 were inactive. These results overall confirmed the binding interaction of the lead compounds with Keap1 protein.

**Quantification of mRNA of Nrf2 Downstream Genes.** To determine whether the compounds activate Nrf2, qRT-PCR was carried out to quantify the mRNA levels of HO-1 and NQO-1 using PC12 cells (Figure 5). HO-1 mRNA was significantly enhanced by compound S47 in dose–response and time–response manners with no obvious effect by the reference compound 3. Noticeably, the HO-1 mRNA was three times of that of compound 3 at 4.5 and 6 h. For NQO-1 mRNA, it was elevated at both doses of S47 but no change at

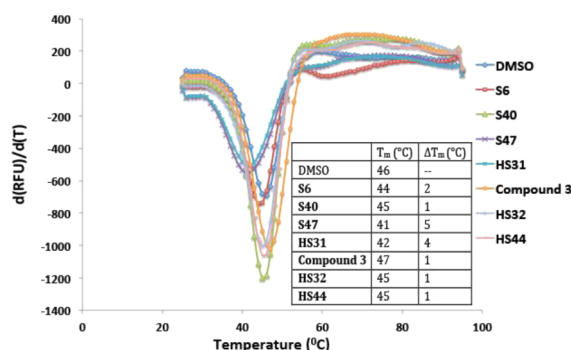


**Figure 4.** Thermal shifts of Keap1 protein with selected compounds (100  $\mu$ M in 0.4% DMSO) determined by DSF assay.

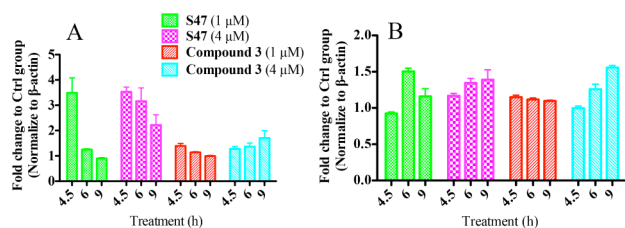


**Figure 5.** The mRNA levels of downstream target genes of Nrf2 measured by qRT-PCR in PC12 cells: (A) HO-1, (B) NQO-1.

low dose of compound 3. These results mechanistically supported our hits disrupting the protein–protein interaction of Keap1 and Nrf2.

**Western Blotting Assay for Nrf2 Nuclear Translocation.** To further validate the mechanism of action, Western blotting was used to characterize the subcellular distribution of Nrf2 protein in PC12 cells. Given that downstream gene up-regulation was observed at 4.5 h (Figure 5), Nrf2 nuclear translocation should occur before that. Indeed, S47 treatment caused a significant decrease in the level of cytosolic Nrf2 protein and an increase in nuclear Nrf2 protein 1.5 h after treatment (Figure 6). The level of Nrf2 protein was reversed after 4.5 h treatment, likely because of the feedback loop of Nrf2 and Keap1 regulation.<sup>21</sup>

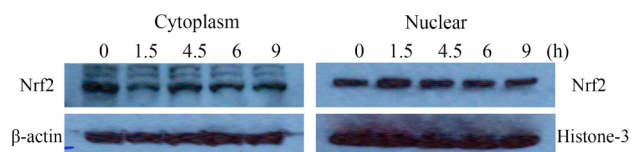


**Figure 6.** Western blotting of S47 (4  $\mu$ M) induced Nrf2 nuclear translocation in PC12 cells.

## CONCLUSION

Three classes of novel inhibitors disrupting Keap1–Nrf2 protein–protein interaction were successfully identified by structure-based virtual screening. Further hit-based substructure search of the potent compounds concluded an informative SAR, which was a high-efficiency strategy and best use of the commercial compound library. Our most potent noncovalent inhibitor exhibits three times improved cellular activation of Nrf2 than the most active noncovalent Keap1 inhibitor known to date. Further cell-based mechanism study supported our new hits disrupting the protein–protein interaction of Keap1 and

Nrf2. Focused medicinal chemistry work is ongoing to expand the SAR of novel inhibitors.

## EXPERIMENTAL SECTION

**Fluorescent Anisotropy Assay.** Determination of equilibrium dissociation constants  $K_D$  for each compound was performed using the fluorescence anisotropy assay with FITC- $\beta$ Ala-DEETGEF-OH (Supporting Information Figure S10) as the fluorescence probe.<sup>10</sup> The fluorescence anisotropy was measured on SpectraMax M5e microplate reader with 485 nm excitation and 535 nm emission after a 60 min incubation at room temperature. The  $K_{D2}$  of each compound tested was determined by fitting the displacement curves as described in the literature<sup>18</sup> (details can be found in Supporting Information).

## ASSOCIATED CONTENT

### Supporting Information

Computational protocols, FITC- $\beta$ Ala-DEETGEF-OH protein sequence and characterization, dose–response curves for inhibition of Keap1–Nrf2 binding of the hits, synthesis of the reference compound, NMR, MS spectra, and HPLC purity of selected compounds. This material is available free of charge via the Internet at <http://pubs.acs.org>.

## AUTHOR INFORMATION

### Corresponding Authors

\*For C.X.: phone, 612-626-5675; fax, 612-624-0139; E-mail, [xingx009@umn.edu](mailto:xingx009@umn.edu).

\*For Y.Y.S.: phone, 612-625-8255; fax, 612-625-8154; E-mail, [shamx002@umn.edu](mailto:shamx002@umn.edu).

### Author Contributions

Ideas and experiment design: C. Zhuang, Y. Y. Sham, C. Xing. Computational development: C. Zhuang, Y. Y. Sham. Chemistry and Biology: C. Zhuang, S. Narayanapillai, C. Xing. Analysis and data interpretation: C. Zhuang, Y. Y. Sham, C. Xing. Writing and review of the manuscript: C. Zhuang, S. Narayanapillai, W. Zhang, Y. Y. Sham, C. Xing. Study supervision: Y. Y. Sham, C. Xing.

### Notes

The authors declare no competing financial interest.

## ACKNOWLEDGMENTS

We thank the Department of Medicinal Chemistry, Minnesota Supercomputing Institute, and the Center for Drug Design for providing the necessary resources. We thank Ran Dai and Dr. Barry Finzel at the University of Minnesota for assistance of DSF assay. We are also grateful to the China Scholarship Council's Ph.D. Abroad Training Plan.

## ABBREVIATIONS USED

NQO-1, NADPH:quinone oxidoreductase 1; HO-1, heme oxygenase-1; SOD, superoxide dismutase; GST, glutathione S-transferase; GPx, glutathione peroxidase; Keap1, Kelch-like ECH-associated protein 1; Nrf2, nuclear factor erythroid 2-related factor 2; ARE, antioxidant response elements; SBVS, structure-based virtual screening; HBSS, hit-based substructure search; SAR, structure–activity relationship; DSF, differential scanning fluorimetry

## REFERENCES

- (1) Uttara, B.; Singh, A. V.; Zamboni, P.; Mahajan, R. T. Oxidative stress and neurodegenerative diseases: a review of upstream and downstream antioxidant therapeutic options. *Curr. Neuropharmacol.* **2009**, *7*, 65–74.

- (2) Dinkova-Kostova, A. T.; Talalay, P. Direct and indirect antioxidant properties of inducers of cytoprotective proteins. *Mol. Nutr. Food Res.* **2008**, *52* (Suppl 1), S128–S138.
- (3) Itoh, K.; Wakabayashi, N.; Katoh, Y.; Ishii, T.; Igarashi, K.; Engel, J. D.; Yamamoto, M. Keap1 represses nuclear activation of antioxidant responsive elements by Nrf2 through binding to the amino-terminal Neh2 domain. *Genes Dev.* **1999**, *13*, 76–86.
- (4) Magesh, S.; Chen, Y.; Hu, L. Small molecule modulators of Keap1–Nrf2–ARE pathway as potential preventive and therapeutic agents. *Med. Res. Rev.* **2012**, *32*, 687–726.
- (5) Prester, T.; Holtzclaw, W. D.; Zhang, Y.; Talalay, P. Chemical and molecular regulation of enzymes that detoxify carcinogens. *Proc. Natl. Acad. Sci. U. S. A.* **1993**, *90*, 2965–2969.
- (6) Wakabayashi, N.; Dinkova-Kostova, A. T.; Holtzclaw, W. D.; Kang, M. I.; Kobayashi, A.; Yamamoto, M.; Kensler, T. W.; Talalay, P. Protection against electrophile and oxidant stress by induction of the phase 2 response: fate of cysteines of the Keap1 sensor modified by inducers. *Proc. Natl. Acad. Sci. U. S. A.* **2004**, *101*, 2040–2045.
- (7) McMahon, M.; Thomas, N.; Itoh, K.; Yamamoto, M.; Hayes, J. D. Redox-regulated turnover of Nrf2 is determined by at least two separate protein domains, the redox-sensitive Neh2 degron and the redox-insensitive Neh6 degron. *J. Biol. Chem.* **2004**, *279*, 31556–31567.
- (8) Lo, S. C.; Li, X.; Henzl, M. T.; Beamer, L. J.; Hannink, M. Structure of the Keap1:Nrf2 interface provides mechanistic insight into Nrf2 signaling. *EMBO J.* **2006**, *25*, 3605–3617.
- (9) Tong, K. I.; Katoh, Y.; Kusunoki, H.; Itoh, K.; Tanaka, T.; Yamamoto, M. Keap1 recruits Neh2 through binding to ETGE and DLG motifs: characterization of the two-site molecular recognition model. *Mol. Cell. Biol.* **2006**, *26*, 2887–2900.
- (10) Inoyama, D.; Chen, Y.; Huang, X.; Beamer, L. J.; Kong, A. N.; Hu, L. Optimization of fluorescently labeled Nrf2 peptide probes and the development of a fluorescence polarization assay for the discovery of inhibitors of Keap1–Nrf2 interaction. *J. Biomol. Screening* **2012**, *17*, 435–447.
- (11) Hu, L.; Magesh, S.; Chen, L.; Wang, L.; Lewis, T. A.; Chen, Y.; Khodier, C.; Inoyama, D.; Beamer, L. J.; Emge, T. J.; Shen, J.; Kerrigan, J. E.; Kong, A. N.; Dandapani, S.; Palmer, M.; Schreiber, S. L.; Munoz, B. Discovery of a small-molecule inhibitor and cellular probe of Keap1–Nrf2 protein–protein interaction. *Bioorg. Med. Chem. Lett.* **2013**, *23*, 3039–3043.
- (12) Marcotte, D.; Zeng, W.; Hus, J. C.; McKenzie, A.; Hession, C.; Jin, P.; Bergeron, C.; Lugovskoy, A.; Enyedy, I.; Cuervo, H.; Wang, D.; Atmanene, C.; Roecklin, D.; Vecchi, M.; Vivat, V.; Kraemer, J.; Winkler, D.; Hong, V.; Chao, J.; Lukashev, M.; Silvian, L. Small molecules inhibit the interaction of Nrf2 and the Keap1 Kelch domain through a non-covalent mechanism. *Bioorg. Med. Chem.* **2013**, *21*, 4011–4019.
- (13) Shoichet, B. K. Virtual screening of chemical libraries. *Nature* **2004**, *432*, 862–865.
- (14) Zhuang, C.; Miao, Z.; Zhu, L.; Dong, G.; Guo, Z.; Wang, S.; Zhang, Y.; Wu, Y.; Yao, J.; Sheng, C.; Zhang, W. Discovery, synthesis, and biological evaluation of orally active pyrrolidone derivatives as novel inhibitors of p53–MDM2 protein–protein interaction. *J. Med. Chem.* **2012**, *55*, 9630–9642.
- (15) Muegge, I. Synergies of virtual screening approaches. *Mini-Rev. Med. Chem.* **2008**, *8*, 927–933.
- (16) Enyedy, I. J.; Egan, W. J. Can we use docking and scoring for hit-to-lead optimization? *J. Comput.-Aided Mol. Des.* **2008**, *22*, 161–168.
- (17) Maggiora, G.; Vogt, M.; Stumpfe, D.; Bajorath, J. Molecular Similarity in Medicinal Chemistry. *J. Med. Chem.* **2013**, DOI: 10.1021/jm401411z.
- (18) Roehrl, M. H.; Wang, J. Y.; Wagner, G. A general framework for development and data analysis of competitive high-throughput screens for small-molecule inhibitors of protein–protein interactions by fluorescence polarization. *Biochemistry* **2004**, *43*, 16056–16066.
- (19) Niesen, F. H.; Berglund, H.; Vedadi, M. The use of differential scanning fluorimetry to detect ligand interactions that promote protein stability. *Nature Protoc.* **2007**, *2*, 2212–2221.
- (20) Wang, L.; Lewis, T.; Zhang, Y. L.; Khodier, C.; Magesh, S.; Chen, L.; Inoyama, D.; Chen, Y.; Zhen, J.; Hu, L.; Beamer, L. J.; Faloon, P. W.; Dandapani, S.; Perez, J. R.; Munoz, B.; Palmer, M.; Schreiber, S. The identification and characterization of non-reactive inhibitor of Keap1–Nrf2 interaction through HTS using a fluorescence polarization assay. In *Probe Reports from the NIH Molecular Libraries Program*; National Institutes of Health: Bethesda, MD, **2010**.
- (21) Lee, O. H.; Jain, A. K.; Papusha, V.; Jaiswal, A. K. An auto-regulatory loop between stress sensors INrf2 and Nrf2 controls their cellular abundance. *J. Biol. Chem.* **2007**, *282*, 36412–36420.